



Cite this: CrystEngComm, 2015, 17,
877

Different solvents yield alternative crystal forms through aromatic, halogen bonding and hydrogen bonding competition†

Solhe F. Alshahateet,*^a Mohan M. Bhadbhade,^b Roger Bishop^c
and Marcia L. Scudder^c

Crystallisation of the racemic V-shaped diquinoline derivative **8** from aprotic dimethyl formamide yields a high symmetry solvent-free crystal structure in space group *Fdd2*. Fully eclipsed columns of enantiomerically pure molecules, joined by *exo*-face to *endo*-face C–H···π and C–H···Cl interactions, are produced. Despite most of the molecular surface being aromatic in nature, classic π···π associations are absent. Adjacent columns of opposite handedness are linked by means of N···Cl and C–H···Cl halogen bonds. In contrast, very different *P2*₁/*c* (**8**)·(solvent) adducts assemble from the protic solvents methanol, ethanol or acetic acid. These isostructural inclusion compounds contain one strong N···H–O hydrogen bond per host molecule, and two such (**8**)·(solvent) units assemble around an inversion centre to form a parallel fourfold aromatic embrace (P4AE) dimer. Its efficient internal *endo,endo*-facial π···π interaction is further supplemented by intra-dimer Cl···π and C–H···Cl associations. These P4AE units are repeated by translation and associate by means of *exo,exo*-facial C–H···Cl rather than π···π interactions, through Cl···π contacts, and by a suite of five host–guest C–H···O weak hydrogen bonds that supplement the N···H–O hydrogen bond. The (**8**)·(acetic acid) structure is notable for the guest carboxylic acid group acting as an alcohol mimic. In this role, the hydroxy group acts in the usual way as a hydrogen bond donor but it is the carbonyl oxygen that functions as the main acceptor atom. These observations illustrate the crucial role that crystallisation solvent choice, and the consequent competing intermolecular associations, play in the production of alternative crystal forms.

Received 20th October 2014,
Accepted 21st November 2014

DOI: 10.1039/c4ce02109f

www.rsc.org/crystengcomm

Introduction

Many compounds are known to be capable of producing more than one crystal form. These alternative solid state assemblies may, for example, be polymorphs,¹ solvates,² hydrates³ or mutually hydrogen bonded co-crystals.⁴ As long ago as 1989 Desiraju highlighted the problems in crystal engineering⁵ that are likely to be caused by polymorphic behaviour,⁶ and a recent report has indicated that over 50% of organic

molecules may form polymorphs.⁷ When the other categories above are also considered, it seems probable that the majority of organic molecules will prove not to have a unique crystal structure if their behaviour is explored thoroughly. The rationalisation and prediction of such crystalline behaviour is a major research area in contemporary chemistry.

For several years we have been exploring the deliberate design of new solvate compounds, particularly those that utilise attractive intermolecular forces weaker than Pauling-type hydrogen bonds. Such crystal engineering remains somewhat problematical, largely because several different types of these weak interactions can act in concert, or in competition, to yield the most favourable result. Nonetheless, the design approach shown in Fig. 1 has proved to be highly effective.⁸ This diagram combines both a specific example (compounds **1–5**),⁹ and also the wider synthetic concept (structures **A–E**).¹⁰ Using the latter symbolism: **A** represents a 2-aminoaryl aldehyde or ketone, **B** a bicyclo[3.3.0]octane- or bicyclo[3.3.1]nonane-2,6- or -3,7-diketone, **C** the pre-host adduct, and **D** & **E** the targeted inclusion host molecules.

^a Department of Chemistry, Faculty of Science, Mutah University, P. O. Box 7, Mutah 61710, Karak, Jordan. E-mail: s.alshahateet@mutah.edu.jo

^b Mark Wainwright Analytical Centre, The University of New South Wales (UNSW), Sydney NSW 2052, Australia

^c School of Chemistry, The University of New South Wales (UNSW), Sydney NSW 2052, Australia

† Electronic supplementary information (ESI) available: Fig. S1 and S2 illustrating the (**8**)·(ethanol) crystal structure. The IR, ¹H NMR and ¹³C NMR spectra of **8** are recorded as Fig. S3–S5, respectively. CCDC 1028008–1028011. For crystallographic information in CIF or other electronic form see DOI: 10.1039/c4ce02109f

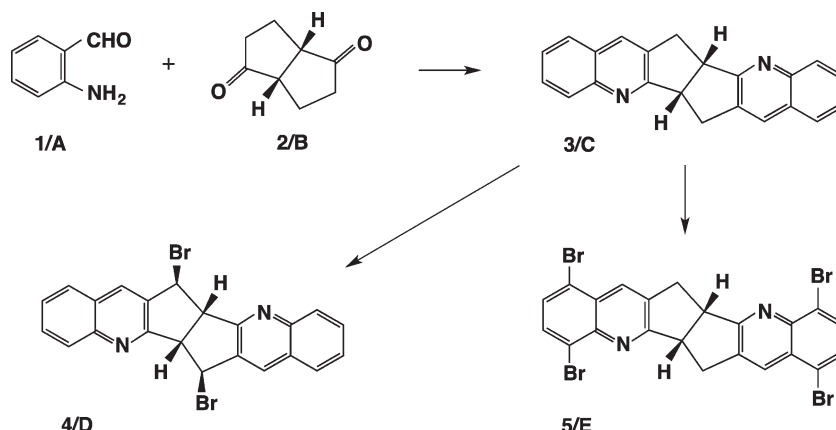


Fig. 1 The synthetic design for preparation of the specific host molecules **4** and **5**; and also their more general relatives **D** and **E**, whose structural characteristics are defined in the text.

This modular synthetic approach has allowed the simple preparation of a wide range of test molecules.

This synthetic design combines three elements, all of which play a vital role in generating the required inclusion properties.

(a) The two diquinoline wings encourage crystal assembly using aryl offset face–face (OFF) and aryl edge–face (EF) interactions.

(b) The central bicyclic ring links these two wings and creates a V-shaped molecule with average C_2 -symmetry in solution. Thus each individual molecule is handed, although the bulk sample is a racemic mixture. The linking ring also permits a certain degree of conformational twisting and flapping, and hence the host can adapt and accommodate guest molecules of differing sizes and shapes.

(c) The halogen substituents (benzylic in **4/D** or aryl in **5/E**) are crucial in attenuating the extent of OFF and EF interactions in the solid state. They act as spoiler groups that restrict the role played by these aromatic forces in three-dimensional crystal propagation. Further, they act as hot spots for host–host and host–guest halogen bonding interactions of various types.

It has been found experimentally that a minimum of four aryl rings is required for the planar wings of **4/D** or **5/E**, and four halogen substituents in **5/E**, for guest inclusion to occur. The level of prediction thus achieved is around 95% and this is unprecedented for weaker interaction compounds. In contrast, the pre-host compounds **3/C** usually yield solvent-free crystals.⁸ This behaviour is examined more closely in the present paper, in which the structural zone between guest inclusion or exclusion has been explored.

Results and discussion

Preparation of the diquinoline derivative **8**

The compound chosen for study was the racemic diquinoline derivative **8**. This was prepared in 93% yield by means of a one-flask acid-catalysed double Friedländer condensation,¹¹ using two equivalents of 2-amino-5-chlorobenzophenone **6** and one of bicyclo[3.3.1]nonane-3,7-dione **7**¹² (Fig. 2).

None of the alternative Friedländer product **9**, which could arise in the second condensation step, was detected. This is in accord with our earlier base catalysed Friedländer condensations employing diketone **7**.¹³ Aguado *et al.*, however, have observed both condensation products when using a different modified Friedländer procedure.¹⁴ In the present case, the isomer **9** would be subject to strong steric crowding effects resulting from the phenyl substituents.

Crystal structure of **8**

Compound **8** is poorly soluble but was crystallised from *N,N*-dimethylformamide (DMF) to give needle crystals suitable

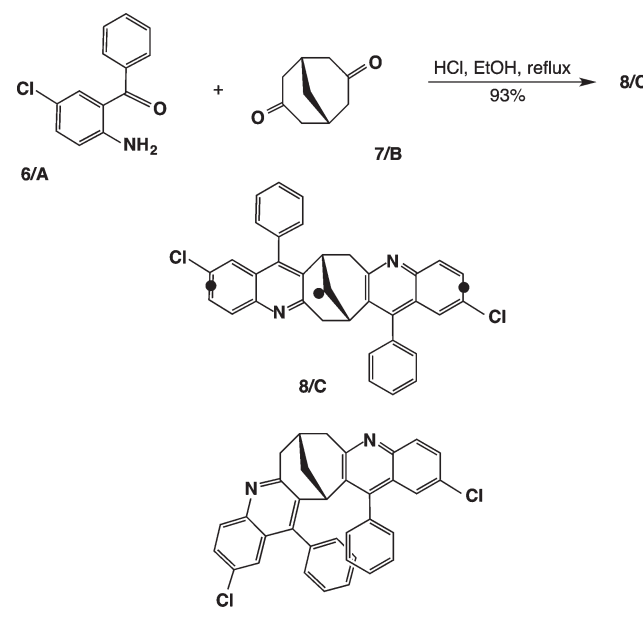


Fig. 2 Preparation of the diquinoline derivative **8** by means of the Friedländer condensation reaction. Only one isomer of the racemic compounds **8**, **9** is illustrated. The black circles added to the molecular structure designate the points used for determining the fold angle (see later) of **8** present in its various crystal structures.

for X-ray structure determination. A solvent-free structure resulted in the orthorhombic space group *Fdd2*. Numerical details of the solution and refinement of this crystal structure (and the others subsequently obtained) are presented in Table 1.

Molecules of **8** stack as fully eclipsed homochiral columns along *c* (Fig. 3, upper). These columns associate as chirally pure layers in the *ac* plane, and these layers have alternating handedness along the *b* direction (Fig. 3, lower). Since each molecule has perfect *C₂* symmetry, only three significant supramolecular interactions are present in this crystal. Each *exo*-wing of **8** subtends two interaction motifs with the *endo*-surface of its neighbour, and there is one motif linking the adjacent layers. Our studies on crystals involving weaker interactions¹⁵ have shown that (as here) their supramolecular synthons¹⁶ are often rather more complex than in crystals that utilise only stronger forces.

The molecular interactions are illustrated in Fig. 4. These zoom-in views emphasise the atoms involved and show only partial molecular structures. The intermolecular *exo,endo*-contact involves a methano hydrogen interacting with both a nitrogen atom and its associated pyridine ring π -system (Fig. 4, left). This bifurcated motif comprises C12–H12A···N1^{17,18} [$d = 2.72 \text{ \AA}$, $D = 3.688(2) \text{ \AA}$, 168.2°] and C12–H12A···C7 (π)¹⁷ [$d = 2.78 \text{ \AA}$] components, the former being more significant based on its good interaction angle. In the second *exo–endo*-motif, phenyl C18–H18···C3 (π benzo ring) [$d = 2.69 \text{ \AA}$], and phenyl C18–H18···Cl1 [$d = 3.04 \text{ \AA}$, $D = 3.716(5) \text{ \AA}$, 130.2°]

interactions operate in concert. The latter contribution appears to be less important considering its poor interaction angle. Neighbouring layers are linked by halogen bonds,¹⁹ comprising a multi-furcated motif composed of C4–Cl1···N1 [3.135(4) \AA , 173.0°] plus four Cl1···H–Ar contacts in the range $d = 2.93$ – 3.08 \AA (Fig. 4, right).

Crystal structures of **8** from methanol, ethanol or acetic acid

In marked contrast, crystallisation of **8** from methanol, ethanol or acetic acid, produced the very different hydrogen bonded adducts (8)·(guest). ORTEP diagrams for these, and the crystallographic numbering system used, are presented in Fig. 5. The host and guest components in these compounds are linked by strong host N···H–O guest hydrogen bonds, and all three of the resulting inclusion structures are essentially isostructural.

Crystal structure of (8)·(methanol)

Crystallisation of **8** from methanol yielded the inclusion compound (8)·(methanol) in space group *P2₁/c*. This crystal structure is completely different from that of pure **8**. The methanol guest forms a hydrogen bond with one of the host nitrogens: O1S–H1S···N2, $D = 2.894(3) \text{ \AA}$. This (8)·(methanol) unit then forms a parallel fourfold aromatic embrace (P4AE) dimer²⁰ with another unit of opposite chirality. The resulting centrosymmetric P4AE dimer is held together by efficient *endo,endo*-facial π ··· π interaction of *ca.* 3.6 \AA (Fig. 6, upper).²¹

Table 1 Numerical details of the solution and refinement of the crystal structures

Crystal form	Apohost	Methanol complex	Ethanol complex	Acetic acid complex
Compound	8	(8)·(Methanol)	(8)·(Ethanol)	(8)·(Acetic acid)
Formula	C ₃₅ H ₂₄ Cl ₂ N ₂	(C ₃₅ H ₂₄ Cl ₂ N ₂)·(CH ₄ O)	(C ₃₅ H ₂₄ Cl ₂ N ₂)·(C ₂ H ₆ O)	(C ₃₅ H ₂₄ Cl ₂ N ₂)·(C ₂ H ₄ O ₂)
Formula mass	543.46	575.50	589.53	603.51
Crystal system	Orthorhombic	Monoclinic	Monoclinic	Monoclinic
Space group	<i>Fdd2</i>	<i>P2₁/c</i>	<i>P2₁/c</i>	<i>P2₁/c</i>
Temperature (K)	223(2)	223(2)	223(2)	223(2)
<i>a</i>	21.2603(17)	10.3943(5)	10.4238(6)	10.4620(5)
<i>b</i>	42.109(4)	17.4818(10)	17.4861(10)	17.5011(8)
<i>c</i> (Å)	5.7891(5)	15.6814(8)	15.9174(8)	15.8272(8)
β (°)	90.00	97.686(1)	98.410(2)	95.530(1)
<i>V</i> (Å ³)	5182.7(7)	2823.9(3)	2870.1(3)	2884.4(2)
<i>Z</i>	8	4	4	4
μ (mm ^{−1})	0.28	0.26	0.26	0.26
Crystal size (mm)	0.66 × 0.09 × 0.09	0.38 × 0.26 × 0.20	0.20 × 0.18 × 0.03	0.40 × 0.40 × 0.30
<i>T</i> _{min} , <i>T</i> _{max}	0.837, 0.975	0.907, 0.949	0.950, 0.992	0.902, 0.925
No. of measured, independent, and observed [<i>I</i> > 2σ(<i>I</i>)] reflections	7385	19 838	15 135	37 577
	2251	6500	4497	6637
	2009	5239	3394	5616
<i>R</i> _{int}	0.054	0.033	0.072	0.023
(sin θ/λ) _{max} (Å ^{−1})	0.595	0.650	0.572	0.650
<i>R</i> [<i>F</i> ² > 2σ(<i>F</i> ²)]	0.067	0.060	0.093	0.048
w <i>R</i> (<i>F</i> ²)	0.144	0.139	0.186	0.135
<i>S</i>	1.23	1.09	1.22	1.05
No. of reflections	2251	6500	4497	6637
No. of parameters	177	375	381	392
No. of restraints	1	0	14	0
Δ> _{max} , Δ> _{min} (e Å ^{−3})	0.43, −0.36	0.32, −0.25	0.47, −0.34	0.38, −0.19
Abs. struct. parameter	−0.07(12)	—	—	—
CCDC number	1028008	1028009	1028010	1028011

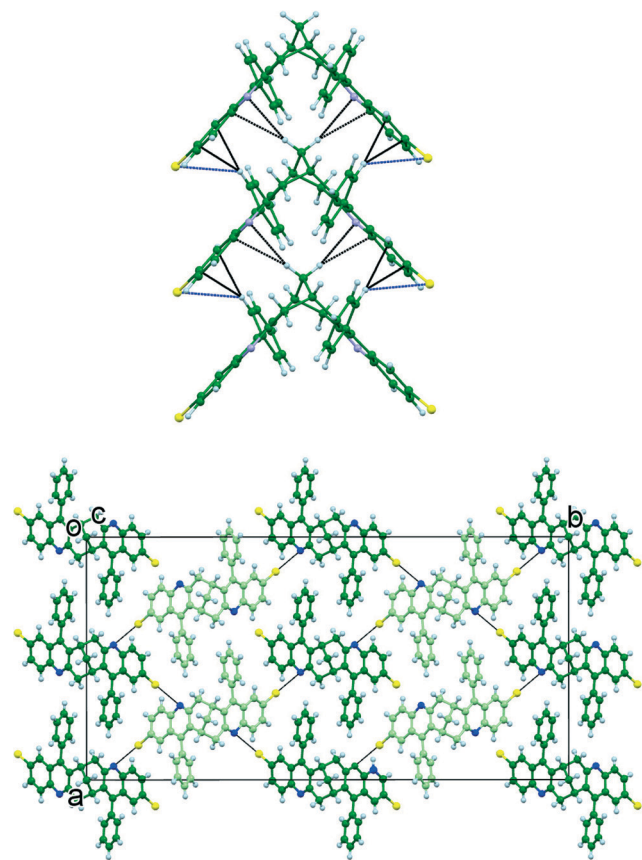


Fig. 3 Upper: the crystal structure of pure **8** showing one stack of homochiral enantiomers along *c*. Lower: layers in the *ac* plane alternate in chirality along the *b* direction. Atom code: C green (opposite enantiomers light or dark), Cl yellow, H light blue and N dark blue.

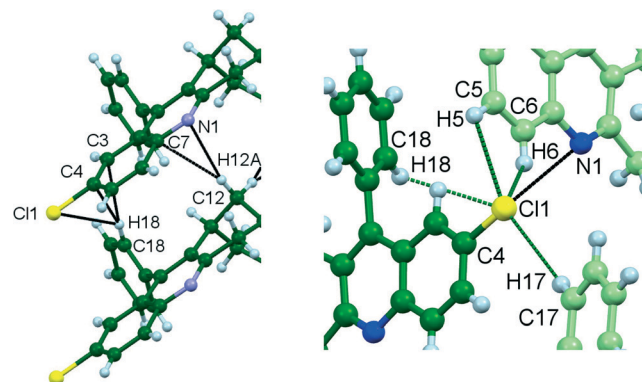


Fig. 4 Left: the intermolecular *exo,endo*-facial contacts present in the crystal structure of **8**. Right: the multi-furcated contacts made by the chlorine substituent with its neighbouring layer. Numerical values are presented in the text.

In addition, $\text{Cl}\cdots\text{H-C}$ (phenyl) and $\text{Cl}\cdots\pi$ (pyridine ring) interactions further link the two (**8**)·(methanol) units, as shown in Fig. 6, lower. The latter motif has a long $\text{Cl}\cdots\text{N}$ contact (3.80 Å) and a poor $\text{C-Cl}\cdots\text{N}$ angle (109°), thus indicating a π interaction rather than a halogen bond. The numerical values of these various interactions are listed in Table 2,

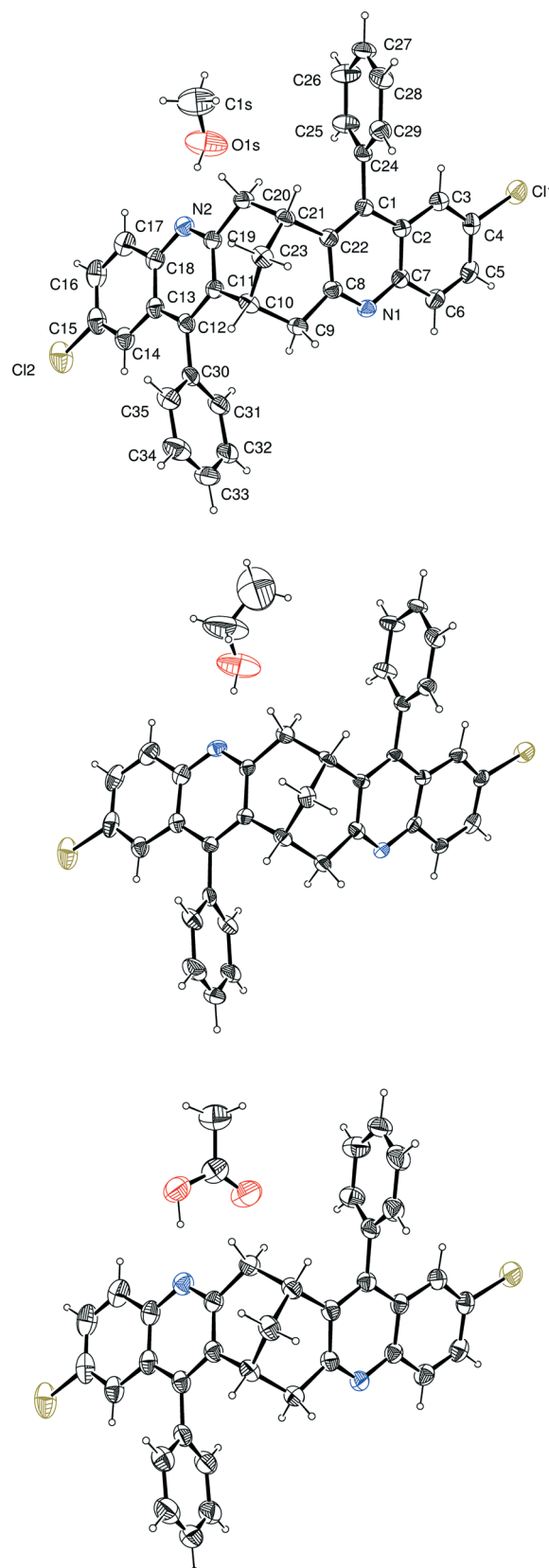


Fig. 5 ORTEP diagrams (ellipsoids drawn at 50% probability level) comparing the three hydrogen bonded (**8**)·(guest) adducts obtained from protic solvents. From top to bottom: the methanol, ethanol, and acetic acid inclusion compounds, respectively. Atom code: C black, O blue and Cl olive.

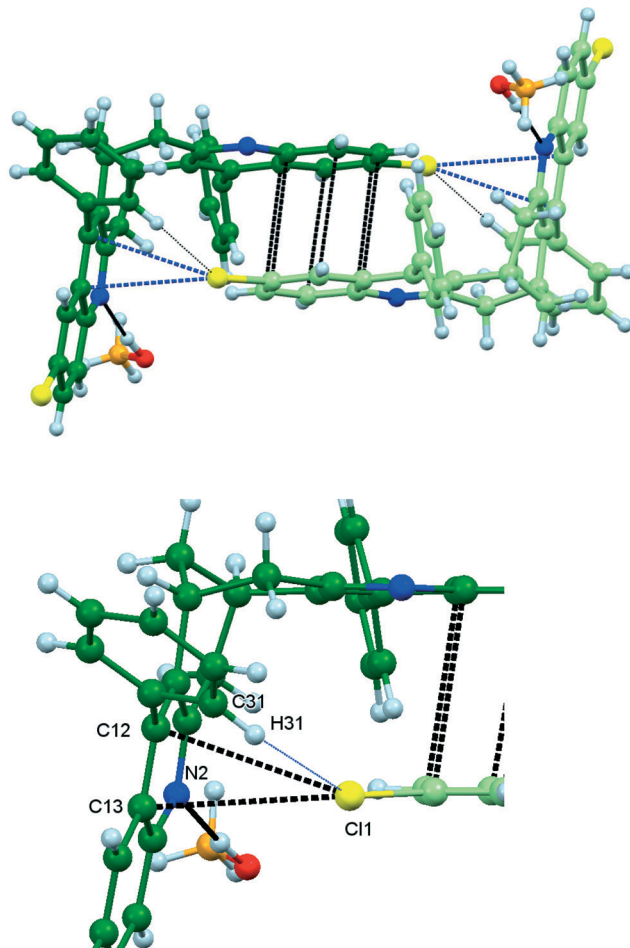


Fig. 6 Upper: the centrosymmetric P4AE dimer formed by host **8** and methanol. Lower: zoom-in view of the intermolecular halogen bonding motif, which comprises $\text{Cl}\cdots\pi$ and $\text{Cl}\cdots\text{H}-\text{C}$ components.

where they are compared with the corresponding values of the ethanol and acetic acid inclusion compounds.

The robust P4AE building blocks are linked into gently undulating chains along the *b* direction (Fig. 7, upper). These chains are translated along *a*, and are repeated in an *ababa* packing sense along *c* where they are cross-linked by $\text{C}-\text{H}\cdots\pi$ and $\text{C}-\text{H}\cdots\text{Cl}\cdots\text{H}$ interactions. Different centrosymmetric *exo,exo*-facial associations join the P4AE dimers, as seen for the projection onto the *ab* plane. At first glance these appear to be conventional $\pi\cdots\pi$ interactions but their aromatic ring separation is poor (only *ca.* 4 Å). Instead, the P4AE units are connected more efficiently through $\text{C}-\text{H}\cdots\text{Cl}$ and $\text{Cl}\cdots\pi$ interactions (Fig. 7, centre). In addition, a phenyl substituent of one molecule participates in a bifurcated $\text{N}1\cdots\text{H}27\cdots\text{Cl}1$ interaction linking two adjacent molecules of **8** along *c* (Fig. 7, lower). Numerical values for these interactions are listed in Table 2.

Crystal structure of (8)-(ethanol)

Compound (8)-(ethanol) is produced when **8** is crystallised from ethanol. This solid is also formed in space group $P2_1/c$

Table 2 Numerical details of the intermolecular attractions for the three inclusion structures

(8)-(Methanol): see Fig. 6 and 7^a

$\pi\cdots\pi$ and $\text{Cl}\cdots\pi$	$X\cdots Y$ (Å)			
Centroid-centroid	3.567(2)			
$\text{Cl}1\cdots\text{C}12^{(i)}$	3.564(2)			
$\text{Cl}1\cdots\text{C}13^{(i)}$	3.601(2)			
$\text{Cl}2\cdots\text{C}32^{(v)}$	3.684(3)			
$\text{Cl}2\cdots\text{C}33^{(v)}$	3.461(3)			
$\text{Cl}2\cdots\text{C}34^{(v)}$	3.673(3)			
$D-\text{H}\cdots A$ (Å)	$D-\text{H}$ (Å)	$H\cdots A$ (Å)	$D\cdots A$ (Å)	$D-\text{H}\cdots A$ (°)
$O1\text{S}-\text{H}1\text{S}\cdots\text{N}2$	0.91	1.95	2.894(3)	170
$C20-\text{H}20\text{A}\cdots\text{Cl}2^{(ii)}$	0.98	3.07	3.968(2)	154
$C27-\text{H}27\cdots\text{N}1^{(iii)}$	0.94	2.64	3.484(3)	149
$C27-\text{H}27\cdots\text{Cl}1^{(iv)}$	0.94	3.08	3.712(2)	126
$C31-\text{H}31\cdots\text{Cl}1^{(i)}$	0.94	2.94	3.760(2)	147

(8)-(Ethanol): see Fig. S1 for the alternative (but equivalent) numbering used^b

$\pi\cdots\pi$ and $\text{Cl}\cdots\pi$	$X\cdots Y$ (Å)			
Centroid-centroid	3.611(2)			
$\text{Cl}2\cdots\text{C}1^{(i)}$	3.617(5)			
$\text{Cl}2\cdots\text{C}2^{(i)}$	3.630(5)			
$\text{Cl}2\cdots\text{C}7^{(i)}$	3.730(5)			
$\text{Cl}1\cdots\text{C}27^{(v)}$	3.376(7)			
$\text{Cl}1\cdots\text{C}28^{(v)}$	3.653(7)			
$D-\text{H}\cdots A$ (Å)	$D-\text{H}$ (Å)	$H\cdots A$ (Å)	$D\cdots A$ (Å)	$D-\text{H}\cdots A$ (°)
$O1\text{S}-\text{H}1\text{S}\cdots\text{N}2$	0.83	2.04	2.858(6)	170
$C9-\text{H}9\text{A}\cdots\text{Cl}1^{(ii)}$	0.98	3.05	3.943(6)	152
$C33-\text{H}33\cdots\text{N}2^{(iii)}$	0.94	2.72	3.548(7)	147
$C33-\text{H}33\cdots\text{Cl}2^{(iv)}$	0.94	3.08	3.723(5)	127
$C25-\text{H}25\cdots\text{Cl}2^{(i)}$	0.94	2.95	3.784(5)	149

(8)-(Acetic acid): see Fig. 8^c

$\pi\cdots\pi$ and $\text{Cl}\cdots\pi$	$X\cdots Y$ (Å)			
Centroid-centroid	3.614(2)			
$\text{Cl}1\cdots\text{C}12^{(i)}$	3.605(2)			
$\text{Cl}1\cdots\text{C}13^{(i)}$	3.635(2)			
$\text{Cl}2\cdots\text{C}32^{(v)}$	3.668(2)			
$\text{Cl}2\cdots\text{C}33^{(v)}$	3.290(2)			
$\text{Cl}2\cdots\text{C}34^{(v)}$	3.570(2)			
$D-\text{H}\cdots A$ (Å)	$D-\text{H}$ (Å)	$H\cdots A$ (Å)	$D\cdots A$ (Å)	$D-\text{H}\cdots A$ (°)
$O2\text{S}-\text{H}2\text{S}\cdots\text{N}2$	0.99	1.72	2.694(3)	169
$C20-\text{H}20\cdots\text{Cl}2^{(ii)}$	0.98	2.72	3.551(2)	147
$C27-\text{H}27\cdots\text{N}1^{(iii)}$	0.94	2.72	3.551(3)	147
$C27-\text{H}27\cdots\text{Cl}1^{(iv)}$	0.94	3.15	3.796(2)	127
$C31-\text{H}31\cdots\text{Cl}1^{(i)}$	0.94	2.88	3.723(2)	150
$C20-\text{H}20\cdots O1\text{S}$	0.98	2.66	3.513(2)	146
$C25-\text{H}25\cdots O1\text{S}$	0.94	2.72	3.339(3)	124

^a (i) $1-x, 2-y, 1-z$ (ii) $1-x, 1-y, 1-z$ (iii) $1+x, y, z$ (iv) $2-x, 2-y, 1-z$ (v) $-x, 1-y, 1-z$. ^b (i) $1-x, 1-y, 1-z$ (ii) $1-x, -y, 1-z$ (iii) $-1+x, y, z$ (iv) $-x, 1-y, 1-z$ (v) $2-x, -y, 1-z$. ^c (i) $2-x, 2-y, 1-z$ (ii) $2-x, 1-y, 1-z$ (iii) $1+x, y, z$ (iv) $3-x, 2-y, 1-z$ (v) $1-x, 1-y, 1-z$.

and is isostructural with the methanol inclusion compound. Illustrations of the (8)-(ethanol) crystal structure are presented as ESI† (Fig. S1 and S2). The numerical values of its intermolecular attractions are listed in Table 2 for comparison with those of the methanol and acetic acid compounds.

Crystal structure of (8)-(acetic acid)

Recrystallisation of **8** from acetic acid yielded (8)-(acetic acid), also in space group $P2_1/c$. This material proved to be

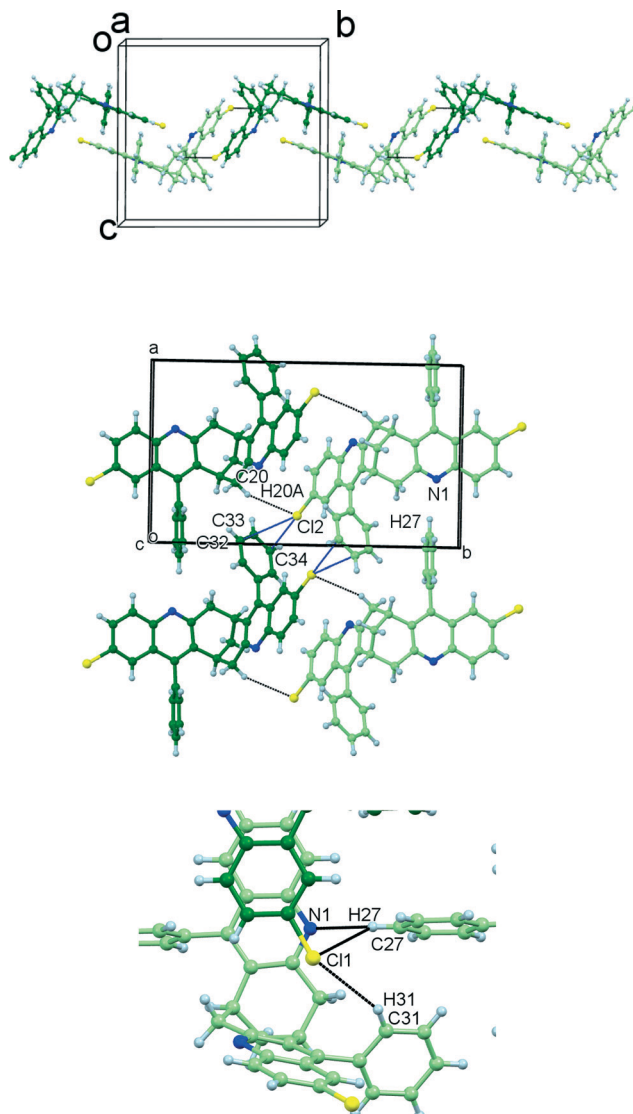


Fig. 7 Upper: part of a chain of host P4AE units running along *b* in (8)-(methanol). Centre: the association of P4AE building blocks showing their effective C–H···Cl interaction and poor π ··· π separation (ca. 4 Å) along *b*, and Cl··· π connectivity along *a*. Lower: zoom-in view of the interaction between molecules of 8 at differing heights down the *c* direction.

surprisingly similar to the two alcohol inclusion compounds and it is essentially isostructural with them (Fig. 8, upper). In part, this is because the guest carbonyl oxygen atom forms C=O···H–C motif links to both host molecules of the P4AE dimer (Fig. 8, lower). The numerical values of the various intermolecular attractions in this crystal structure are described in Table 2.

Comparison of the crystal structures

The molecular structure of 8 has a slightly twisted V-shape and it is capable of limited conformational mobility. We use the fold angle (defined in Fig. 2) to measure such variations in behaviour. The observed angles for the four crystal

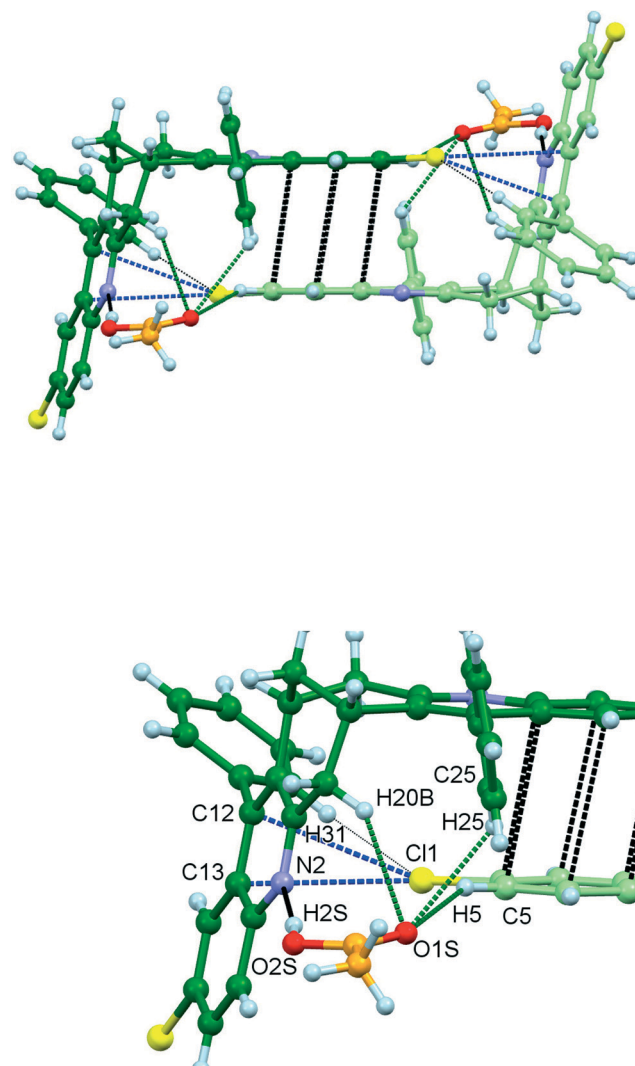


Fig. 8 Upper: the centrosymmetric P4AE dimer building block formed by host 8 and acetic acid. Lower: close-up view of the intermolecular attractions holding the corners of the dimer together. The contributing role of the guest carbonyl oxygen O1S should be particularly noted.

structures (Table 3) are within the routine range for related molecules. However, the value for pure 8 (83.7°) is significantly smaller than the consistent angles (95.8 – 96.0°) observed for the three inclusion structures. This is necessary to achieve the observed fully eclipsed packing arrangement of molecules in the solvent-free crystal structure.

Calculated densities for the crystals (Table 3) lie between 1.354 and 1.393 g cm^{-3} . The values for the methanol and ethanol compounds are similar (1.354 and 1.364), and those for the acetic acid compound and pure 8 are close to each other (1.390 and 1.393 g cm^{-3} , respectively). Direct comparisons are invalid since the four materials have differing molecular formulae: unlike solvent-free 8, the three inclusion materials contain oxygenated guests. Nonetheless, the highest density value is that of pure 8. The packing coefficients provide a fairer means of comparison. It turns out that pure 8 has an almost identical value to its two alcohol

Table 3 Molecular parameters for the diquinoline derivative **8** in its four crystal structures

Compound	8	(8)·(Methanol)	(8)·(Ethanol)	(8)·(Acetic acid)
Fold angle ^a (°)	83.7	96.0	95.8	96.0
Calculated density (g cm ⁻³)	1.393	1.354	1.364	1.390
Packing coefficient (%)	69.2	69.5	69.3	68.3

^a As defined on molecular structure **8** in Fig. 2.

inclusion compounds. That for the acetic acid compound is marginally lower (Table 3).

Crystal lattice energy calculations were performed using the Cerius² ® package,²² which gave the lattice packing energy per mole of unit cells (Table 4). Since the bigger the volume considered, the larger the energy value obtained, correction to a common standard volume is necessary for a meaningful comparison. Here, the total energy was divided by the unit cell volume/1000, which is equivalent to normalising all four structures at a common volume of 1000 Å³. Solvent-free **8** has the highest relative energy ($-119.0 \text{ kcal mol}^{-1}$), as would be anticipated from its experimental willingness to form inclusion structures. The methanol ($-144.2 \text{ kcal mol}^{-1}$) and ethanol ($-146.4 \text{ kcal mol}^{-1}$) inclusion compounds have almost identical values, and these are slightly lower than the acetic acid compound ($-137.4 \text{ kcal mol}^{-1}$).

These data show that although pure **8** has a high symmetry crystal structure, with efficient density and packing coefficient values, it actually has the least favourable crystal packing energy. Possible reasons for this situation are now discussed.

Why is the inclusion crystal form better?

First, it should be noted that molecules of our general structure C (the ‘pre-hosts’) are not normally expected to exhibit inclusion properties, although we have found exceptions.²³ Isolation of solvent-free crystalline **8** from the aprotic solvent DMF was therefore less surprising than the observation of the three cases of protic guest inclusion. The orientation of the substituent phenyl rings is essentially unchanged across the four crystal structures. Pure **8** has an asymmetric unit containing only half a molecule and adopts the higher symmetry space group *Fdd2*. This crystal structure appears ideal at first sight, but contains inherent weaknesses that are absent in the inclusion structures. These have an asymmetric

unit containing a complete molecule of both **8** and the guest and crystallise in the lower symmetry space group *P2₁/c*.

Our molecular design of the general structures C–E utilises V-shaped molecules that are also chiral. The three common means of packing two such molecules are shown diagrammatically in Fig. 9. These are **F** *endo,exo*-, **G** *endo,endo*-, and **H** *exo,exo*-facial packing, respectively. The first of these **F**, observed in the crystal structure of pure **8**, is relatively uncommon since it is preferred for the participating molecules to have the same handedness for this *endo,exo*-facial packing to be efficient. Otherwise there is a mismatch (and poorer interaction) between the adjacent molecules. The crystal structure of solvent-free **8** (Fig. 3) is a textbook example of *endo,exo*-facial packing: the stacked molecules are homochiral, have perfect *C₂*-symmetry and are completely eclipsed.

These characteristics are also a liability. Considerable enantiomeric ordering is necessary during crystallisation to produce the stacks of homochiral enantiomers on which the structure depends. This enantiomer ordering phenomenon is a fascinating aspect of chemistry that has received surprisingly little attention from the crystal engineering community so far.²⁴ This requirement comes at considerable entropic cost. Fig. 10 shows the molecular packing of pure **8** and (**8**)·(methanol), each projected onto the *ab* plane, and provides a clear visual comparison of their entirely different degrees of enantiomer ordering.

The aromatic planes in **F**, and the crystal structure of pure **8**, are aligned ideally parallel to each other. However, their separation in pure **8** is *ca.* 4.1 Å, rather than the 3.5–3.6 Å value usually observed for efficient π···π interaction. This situation arises from the presence of the hydrogen atoms that participate in *exo,endo*-intermolecular C–H···π associations (Fig. 3). Hence the attractive energy provided by π···π interaction is low, despite most of the surface of the molecule **8** being aromatic.

Table 4 Energy (kcal mol⁻¹) and molecular packing calculations for **8** and its inclusion compounds

Compound	8	(8)·(Methanol)	(8)·(Ethanol)	(8)·(Acetic acid)
Van der Waals energy	-433.2	-230.8	-253.2	-207.4
Coulombic energy (QE _q)	-183.7	-162.1	-153.1	-174.7
Hydrogen bonding energy	—	-14.2	-14.0	-14.3
Total energy ^a	-616.9	-407.1	-420.3	-396.4
Unit cell volume (Å ³)	5182.7	2823.9	2870.1	2884.4
Relative packing energy ^b	-119.0	-144.2	-146.4	-137.4

^a Calculated crystal packing energy (kcal mol⁻¹ of unit cells). ^b Total energy ÷ unit cell volume/1000. (Packing energy per 1000 Å³ of the crystal).

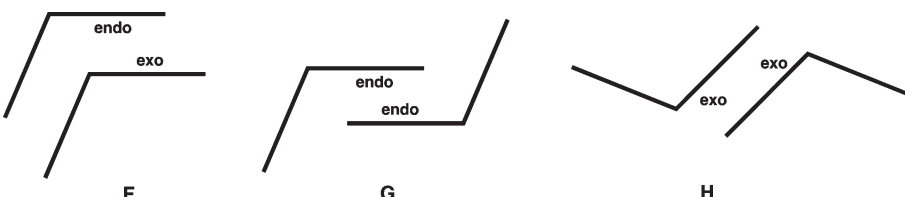


Fig. 9 Diagrammatic representation of the common packing interaction orientations of two V-shaped molecules.

This limitation is removed in the isostructural series of inclusion compounds. Every host molecule in these crystals participates in *endo,endo*- $\pi\cdots\pi$ interaction G (Fig. 6, S1† and 8). Further, these interactions surround an inversion centre and therefore the opposite enantiomers are in intimate association: no energetically costly enantiomer separation is necessary. *Exo,exō*-facial packing H is also present in the inclusion structures but, once again, the $\pi\cdots\pi$ separation is long (*ca.* 4 Å). A high degree of competition between the various aromatic and halogen bonding interaction possibilities is in play, and the dominant interactions in this case are C–H \cdots Cl and C–H \cdots π interactions surrounding inversion centres (Fig. 7). It is also worth noting that the N \cdots Cl halogen bond used in pure solid 8 is absent in its inclusion structures.

Earlier, we remarked that molecules utilising weaker packing forces often tend to use more complex supramolecular

synths in their crystals.¹⁵ There is a considerably increased tendency for multi-atom associations and multi-furcated motifs to occur. Several additional examples have been described here. This phenomenon presents big challenges, but also new opportunities, for the systematic crystal engineering of weaker force compounds. In this context, the host–guest interaction in the present inclusion compounds requires closer examination.

The host–guest environment in (8)·(methanol) is explored in Fig. 11. It reveals that the guest methanol links two host 8 molecules of the same chirality: the one to which it is joined by N \cdots H–O hydrogen bonding, and its neighbour in the adjacent chain running along *b*. Five host–guest C–H \cdots O contacts are present in the range *d* = 2.81 to 3.03 Å. Although some of these values are a bit high, this pattern is duplicated exactly in (8)·(ethanol) (Fig. S2†) and closely followed in the (8)·(acetic acid) crystal.

The (8)·(acetic acid) crystal has a host–guest interaction pattern that is slightly different, but nonetheless remarkably similar, to the alcohol cases (Fig. 12). Once again, the N \cdots H–O hydrogen bond is supplemented by five C–H \cdots O weak hydrogen bonds. The intermolecular connectivity now differs, however, with the guest linking three host molecules. The hydroxy group oxygen accepts only one C–H hydrogen atom, and the carbonyl oxygen accepts the other four.

The preference for alcohol hydroxy groups forming hydrogen bonded chains and rings is well known: the hydroxy hydrogen is the donor, while the alcohol oxygen atom acts as the acceptor.²⁵ It is less well known that the carboxylic acid group can sometimes function like an extended alcohol hydroxy group or alcohol mimic. In such circumstances, the hydroxy hydrogen remains the donor but the carbonyl oxygen atom becomes the acceptor.²⁶ This is the role the acetic acid guest is playing in the (8)·(acetic acid) crystal, and it explains why almost all the C–H \cdots O weak hydrogen bonds are now accepted by the carbonyl oxygen.

It should be noted that the atomic displacement parameter (ADP) values of the methanol and ethanol guests are large compared to the atoms of the host molecule (and also those of the guest acetic acid). The methanol and ethanol molecules are attached to the host through only their hydroxy group. This single-point attachment means that the guest can move slightly in a pendulum-like manner. The larger ethanol has additional conformational possibilities and consequently its ADP values are greater. In contrast, the acetic acid molecule is connected to the host by two-point attachment (through the hydroxy and carbonyl oxygen groups). Its

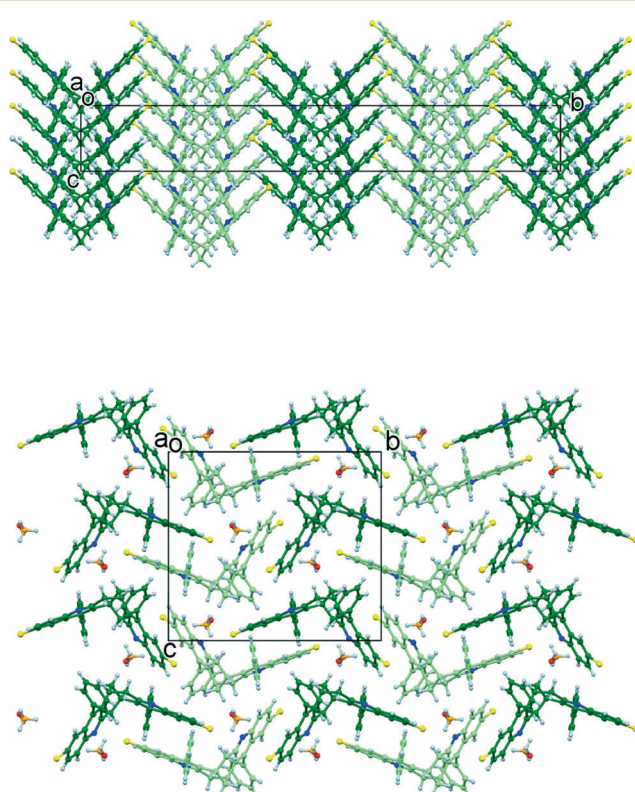


Fig. 10 The crystal structures of pure 8 (upper), and (8)·(methanol) (lower), each projected onto the *ab* plane and with the opposite enantiomers coloured dark or light green. The contrast between the high and low degrees of enantiomer ordering in the two respective solids is striking.

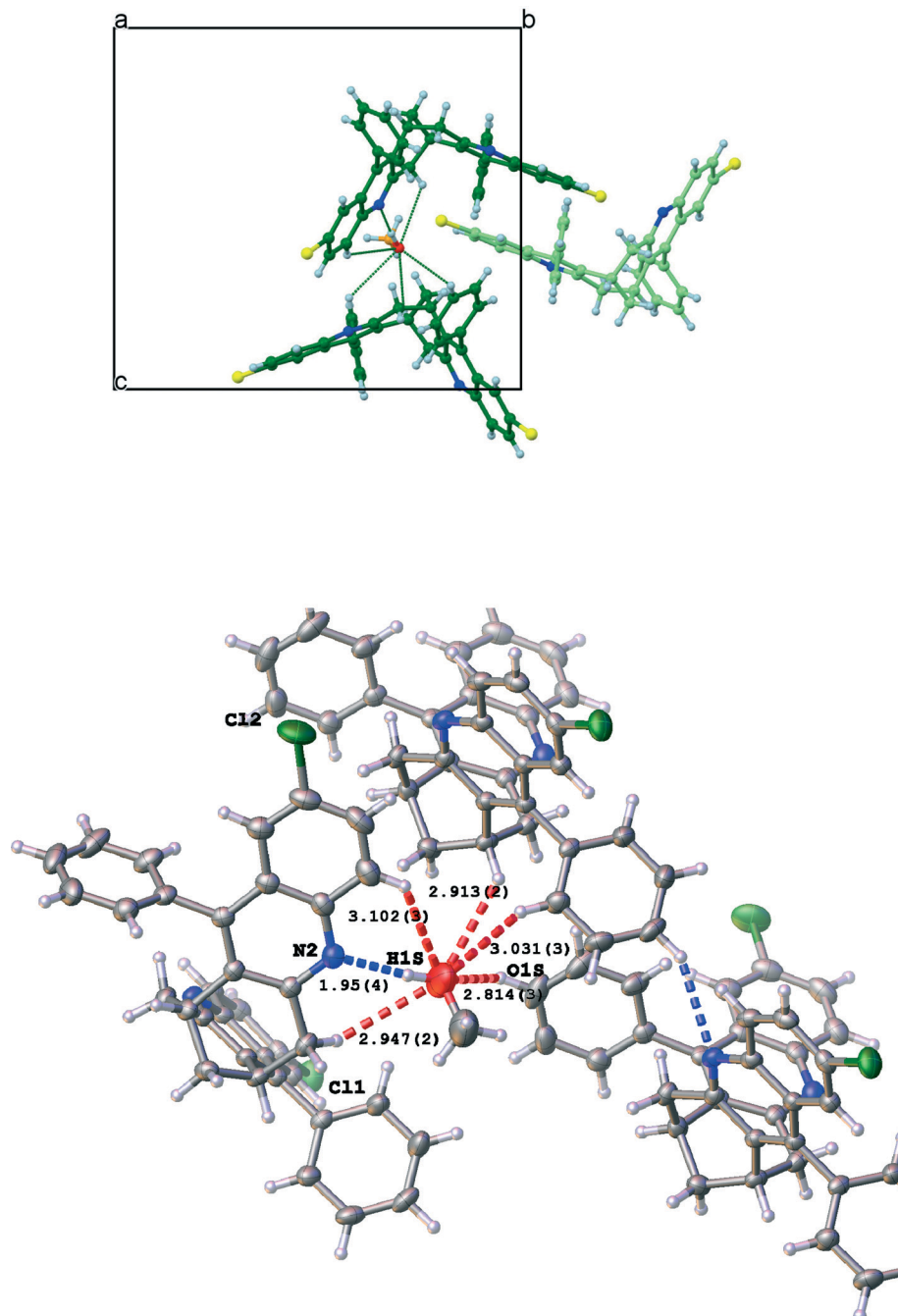


Fig. 11 The host–guest region of the (8·methanol) crystal structure. Upper: the host–guest intermolecular contacts between two P4AE dimers in adjacent chains. Lower: the N···H–O strong hydrogen bond (blue) and five C–H···O weak hydrogen bonds (red) present. A host–host C–H···N (blue) connection is also indicated.

motion is thereby considerably reduced and this results in a remarkably ordered combination.

Concluding remarks

We have observed previously that, as expected, the isomeric diphenyl derivatives **10**²⁷ and **11**²⁸ (Fig. 13) showed no evidence of inclusion properties. This was also the case for the dichloro diphenyl compound **12**,²⁹ and therefore we were

surprised to obtain the present inclusion compounds from its isomer **8**. Solvent-free **12** crystallised in an entirely different manner to **8**: its racemate underwent spontaneous resolution to produce a crystalline conglomerate in space group *P*2₁. Molecules **8** and **12** occupy a fascinating border area between guest exclusion or inclusion, and so are worthy of further investigation.

Our results reveal that the guest molecules in these compounds of **8** fit snugly within the crystal structures and

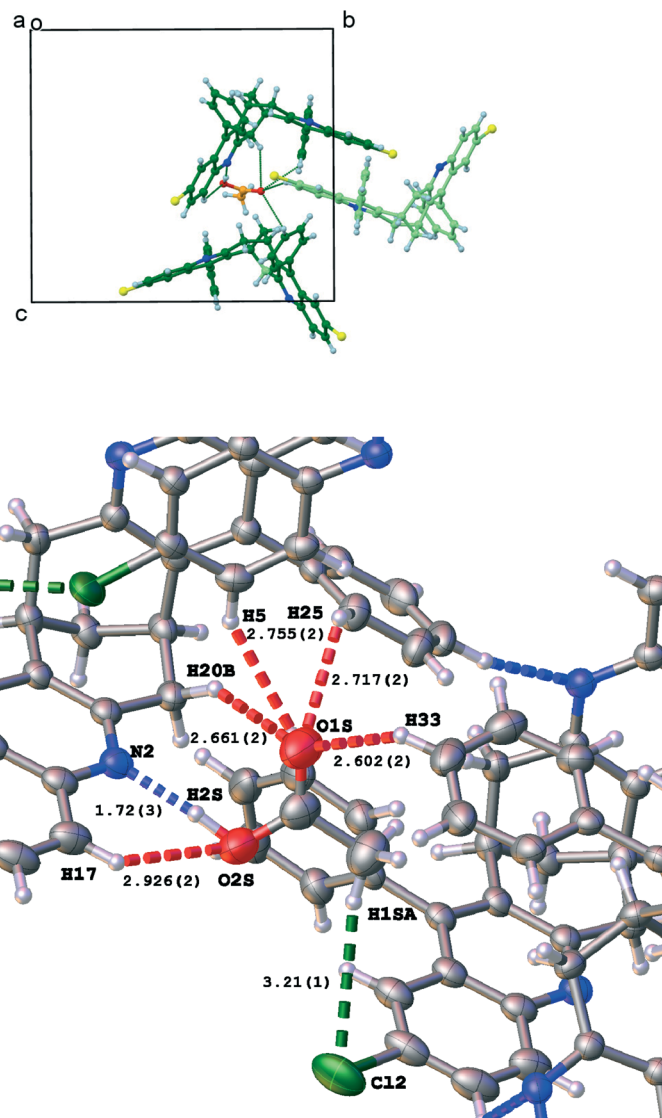


Fig. 12 The spectrum of host–guest hydrogen bonding interactions present in (8)–(acetic acid). Upper: the host–guest intermolecular contacts between three host molecules. Lower: the N···H–O strong hydrogen bond and five C–H···O weak hydrogen bonds (red) formed using both the hydroxy and carbonyl oxygen atoms of the acetic acid guest. A host–host C–H···N (blue) and two host–host C–H···Cl (green) connections are also indicated.

play a more fundamental structural role than is at first apparent. The choice of crystallisation solvent is revealed to be of subtle, but highly profound, importance. Different combinations of competing molecular interaction types can result in very different crystal forms of the solute being produced.

Experimental

The m.p. was determined on a Stuart scientific melting point apparatus (open capillary tube) and the FTIR spectrum recorded on a Maltson 5000 FTIR spectrophotometer. NMR data were obtained using a Bruker 500 MHz Avance III instrument at The University of Jordan. Chemical shifts were referenced to TMS as the internal standard and CDCl_3 as the solvent. Carbon substitution was determined using the DEPT

procedure. Electrospray HRMS data were recorded using a Finnigan/MAT 95XL-T mass spectrometer. The X-ray single crystal structure determinations were carried out at The National University of Singapore.

2,10-Dichloro-8,16-diphenyl-6,7,14,15-tetrahydro-7,15-methanocycloocta[1,2-*b*:5,6-*b'*]diquinoline 8

2-Amino-5-chlorobenzophenone **6** (0.42 g, 1.8 mmol) and bicyclo[3.3.1]nonane-3,7-dione **7**¹² (0.13 g, 0.89 mmol) were dissolved in ethanol (20 mL) and HCl (10 M, 2 mL) was added. The mixture was then refluxed overnight. The resulting precipitate was filtered and washed with ice-cold ethanol to yield the diquinoline **8** as an off-white solid (0.45 g, 93%), m.p. 260 °C (decomp). IR ν_{max} (paraffin mull)

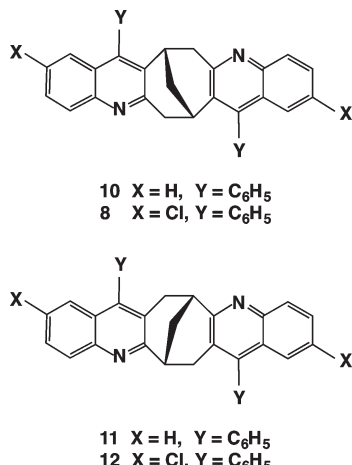


Fig. 13 Molecular structures of the related diheteroaromatic molecules **8** and **10–12**. Only one enantiomer of the racemic material used is shown.

3064, 2952, 2870, 2823, 1639, 1600, 1580, 1518, 1474, 1378, 1224, 1168, 1074, 1028, 973, 952, 835, 757, 730, 700, 617, 564 cm⁻¹ (Fig. S3†). ¹H NMR (CDCl₃) δ 2.33 (br s, 2H, bridging CH₂), 3.31–3.36 (dd, *J*_{AB} = 18.6 Hz, *J*_{AX} = 5.9 Hz, 2H), 3.58 and 3.61 (d, *J*_{AB} = 18.6 Hz, 2H), 3.76 (br s, 2H), 7.26–7.27 (m, 2H), 7.29–7.30 (m, 2H), 7.57–7.63 (m, 8H), 7.75–7.79 (m, 2H), 8.27 (d, *J* = 8.1 Hz, 2H) (Fig. S4†). ¹³C NMR (CDCl₃) δ 28.30 (CH₂), 28.94 (CH), 40.08 (CH₂), 125.27 (CH), 126.64 (CH), 128.02 (CH), 128.35 (C), 129.26 (CH), 129.35 (CH), 129.67 (CH), 129.70 (CH), 132.18 (CH), 132.56 (C), 133.59 (C), 133.88 (C), 141.11 (C), 151.31 (C), 154.92 (C) (Fig. S5†). HRMS (ESI, *m/z*⁺): calc. for ¹²C₃₅H₂₄³⁵Cl₂N₂ 542.1311, found 542.1324; calc. for ¹²C₃₄¹³C₁H₂₄³⁵Cl₂N₂ 543.1345, found 543.1386; calc. for ¹²C₃₅H₂₄³⁵Cl₁³⁷Cl₁N₂ 544.1281, found 544.1407; calc. for ¹²C₃₄¹³C₁H₂₄³⁵Cl₁³⁷Cl₁N₂ 545.1315, found 545.1377; calc. for ¹²C₃₅H₂₄³⁷Cl₂N₂ 546.1252, found 546.1408.

Structure determinations

Reflection data were measured at 223(2) K on a Bruker SMART APEX-1000 diffractometer equipped with a CCD detector and Mo-Kα sealed tube. SMART was used for collecting frame data, indexing reflection, determination of lattice parameters, integration of intensity of reflections and scaling.³⁰ SADABS was used for absorption correction³¹ and SHELLXTL for space group, structure determination, and least-square refinements on *F*².³² All the hydrogen atoms were treated using riding model approximation, except the H-atoms of the OH groups. These H-atoms located in the difference Fourier were allowed to refine freely with their isotropic temperature factors in the full matrix least-squares refinement.

Energy calculations

Intermolecular potential for atoms *i*, *j* with charges *q_i*, *q_j* separated by *d_{ij}* is given by eqn (1), and comprises the van der Waals and coulombic energies. The atom parameters *e^a* (kcal mol⁻¹), *r^a* (Å), are: C, 0.095, 1.95; N, 0.077, 1.83;

H, 0.015, 1.60; Cl 0.283, 1.98; O 0.096, 1.70. The combination rules are given in eqn (2) and (3). The permittivity *ε* in eqn (1) = 1.

$$E_{ij} = e_{ij}^a [(d_{ij}/d_{ij}^a)^{-12} - 2(d_{ij}/d_{ij}^a)^{-6}] + (q_i q_j)/(\epsilon \cdot d_{ij}) \quad (1)$$

$$d_{ij}^a = r_i^a + r_j^a \quad (2)$$

$$e_{ij}^a = (e_i^a \cdot e_j^a)^{0.5} \quad (3)$$

Atom partial charges *q* were calculated using the QE procedure of Rappe and Goddard,³³ as implemented in the MSI Cerius² ® software.²² This method of equalisation of chemical potential is responsive to geometry. The lattice energy computed was normalised to allow for variation in cell volume: the values quoted are energy per 1000 Å³. This compensates for the fact that the energy calculations for the different structures incorporated different numbers of atoms.

References

- (a) J. Bernstein, R. J. Davey and J.-O. Hencke, *Angew. Chem., Int. Ed.*, 1999, **38**, 3440–3461; (b) J. Bernstein, *Polymorphism in Molecular Crystals*, Oxford Science Publications, Oxford, 2002; (c) D. Braga, L. Brammer and N. R. Champness, *CrystEngComm*, 2005, **7**, 1–5; (d) A. Nangia, *Acc. Chem. Res.*, 2008, **41**, 595–604; (f) K. Fucke, N. Qureshi, D. S. Yufit, J. A. K. Howard and J. W. Steed, *Cryst. Growth Des.*, 2010, **10**, 880–886.
- (a) F. H. Herbstein, *Crystalline Molecular Complexes and Compounds: Structures and Principles*, Oxford University Press, Oxford, 2005; (b) S. Varughese and S. M. Draper, *Cryst. Growth Des.*, 2010, **10**, 2571–2580; (c) R. Bishop, Synthetic Clathrate Systems, in *Supramolecular Chemistry: From Molecules to Nanomaterials*, ed. P. A. Gale and J. W. Steed, Wiley, Chichester, 2012, pp. 3033–3056.
- (a) G. R. Desiraju, *J. Chem. Soc., Chem. Commun.*, 1991, 426–428; (b) R. Custelcean, C. Afloroaei, M. Vlassa and M. Polverejan, *Angew. Chem., Int. Ed.*, 2000, **39**, 3094–3096; (c) M. Mascal, L. Infantes and J. Chisholm, *Angew. Chem., Int. Ed.*, 2006, **45**, 32–36; (d) J. Van de Streek, *CrystEngComm*, 2007, **9**, 350–352; (e) B. C. R. Sansam, K. M. Anderson and J. W. Steed, *Cryst. Growth Des.*, 2007, **7**, 2649–2653; (f) L. Infantes, L. Fabian and W. D. S. Motherwell, *CrystEngComm*, 2007, **9**, 65–71.
- (a) F. Lara-Ochoa and G. Espinosa-Pérez, *Supramol. Chem.*, 2007, **19**, 553–557; (b) M. J. Zaworotko, *Cryst. Growth Des.*, 2007, **7**, 4–9; (c) N. Shan and M. J. Zaworotko, *Drug Discovery Today*, 2008, **13**, 440–446; (d) T. Friscic and W. Jones, *Cryst. Growth Des.*, 2009, **9**, 1621–1637; (e) J. H. Ter Horst, M. A. Deij and P. W. Cains, *Cryst. Growth Des.*, 2009, **9**, 1531–1537; (f) K. M. Anderson, M. R. Probert, C. N. Whiteley, A. M. Rowland, A. E. Goeta and J. W. Steed, *Cryst. Growth Des.*, 2009, **9**, 1082–1087.
- (a) G. R. Desiraju, *Crystal Engineering: The Design of Organic Solids*, Elsevier, Amsterdam, 1989; (b) G. R. Desiraju,

- J. J. Vittal and A. Ramanan, *Crystal Engineering: A Textbook*, World Scientific, New Jersey, 2011; (c) R. Bishop, Crystal Engineering, in *Kirk-Othmer Encyclopedia of Chemical Technology*, Wiley, Hoboken, 2014, pp. 1–31, DOI: 10.1002/0471238961.
- 6 G. R. Desiraju, *Polymorphism – the Nemesis of Crystal Design?*, in ref. 5a, 1989, ch. 10, pp. 285–301.
- 7 G. P. Stahly, *Cryst. Growth Des.*, 2007, 7, 1007–1026.
- 8 (a) C. E. Marjo, A. N. M. M. Rahman, R. Bishop, M. L. Scudder and D. C. Craig, *Tetrahedron*, 2001, 57, 6289–6293; (b) R. Bishop, Supramolecular Host-Guest Chemistry of Heterocyclic V-shaped Molecules, *Top. Heterocycl. Chem.*, 2009, 18, 37–74; (c) R. Bishop, *Aust. J. Chem.*, 2012, 65, 1361–1370.
- 9 (a) A. N. M. M. Rahman, R. Bishop, D. C. Craig and M. L. Scudder, *Chem. Commun.*, 1999, 2389–2390; (b) A. N. M. M. Rahman, R. Bishop, D. C. Craig and M. L. Scudder, *CrystEngComm*, 2002, 4, 510–513; (c) A. N. M. M. Rahman, R. Bishop, D. C. Craig and M. L. Scudder, *Eur. J. Org. Chem.*, 2003, 72–81; (d) A. N. M. M. Rahman, R. Bishop, R. Tan and N. Shan, *Green Chem.*, 2005, 7, 207–209.
- 10 (a) A. N. M. M. Rahman, R. Bishop, D. C. Craig, C. E. Marjo and M. L. Scudder, *Cryst. Growth Des.*, 2002, 2, 421–426; (b) A. N. M. M. Rahman, R. Bishop, D. C. Craig and M. L. Scudder, *CrystEngComm*, 2003, 5, 422–428; (c) A. N. M. M. Rahman, R. Bishop, D. C. Craig and M. L. Scudder, *Org. Biomol. Chem.*, 2004, 2, 175–182.
- 11 (a) C.-C. Cheng and S.-J. Yan, *Org. React.*, 1982, 28, 37–201; (b) R. P. Thummel, *Synlett*, 1992, 1–12.
- 12 S. H. Bertz, *J. Org. Chem.*, 1985, 50, 3585–3592.
- 13 (a) S. F. Alshahateet, R. Bishop, D. C. Craig and M. L. Scudder, *Cryst. Growth Des.*, 2004, 4, 837–844; (b) S. F. Alshahateet, N. M. Alghezawi and R. Bishop, *Jordan J. Chem.*, 2011, 6, 139–151.
- 14 F. Aguado, A. Badía, J. E. Baños, F. Bosch, C. Bozzo, P. Camps, J. Contreras, M. Dierssen, C. Escalano, D. M. Gorbig, D. Muñoz-Torrero, M. D. Pujol, M. Simón, M. T. Vázquez and N. M. Vivas, *Eur. J. Med. Chem.*, 1994, 29, 205–221.
- 15 (a) S. F. Alshahateet, R. Bishop, M. L. Scudder, C. Y. Hu, E. H. E. Lau, F. Kooli, Z. M. A. Judeh, P. S. Chow and R. B. H. Tan, *CrystEngComm*, 2005, 7, 139–142; (b) J. Gao, M. M. Bhadbhade and R. Bishop, *CrystEngComm*, 2012, 14, 138–146; (c) V. Suryanti, M. Bhadbhade, R. Bishop, D. S. Black and N. Kumar, *CrystEngComm*, 2012, 14, 7345–7354.
- 16 (a) G. R. Desiraju, *Angew. Chem., Int. Ed. Engl.*, 1995, 34, 2328–2361; (b) A. Mukherjee, K. Dixit, S. P. Sarma and G. R. Desiraju, *IUCrJ*, 2014, 1, 228–239.
- 17 G. R. Desiraju and T. Steiner, *The Weak Hydrogen Bond in Structural Chemistry and Biology*, Oxford University Press, Oxford, 1999.
- 18 (a) S. F. Alshahateet, R. Bishop, D. C. Craig and M. L. Scudder, *CrystEngComm*, 2001, 3(48), 225–229; (b) C. E. Marjo, R. Bishop, D. C. Craig and M. L. Scudder, *Eur. J. Org. Chem.*, 2001, 863–873.
- 19 (a) P. Metrangolo, H. Neukirch, T. Pilati and G. Resnati, *Acc. Chem. Res.*, 2005, 38, 386–395; (b) P. Metrangolo, F. Meyer, T. Pilati, G. Resnati and G. Terraneo, *Angew. Chem., Int. Ed.*, 2008, 47, 6114–6127; (c) C. E. Marjo, R. Bishop, D. C. Craig, A. O'Brien and M. L. Scudder, *J. Chem. Soc., Chem. Commun.*, 1994, 2513–2514; (d) P. Metrangolo and G. Resnati, *IUCrJ*, 2014, 1, 5–7.
- 20 (a) I. Dance and M. Scudder, *J. Chem. Soc., Chem. Commun.*, 1995, 1039–1040; (b) I. Dance and M. Scudder, *Chem. – Eur. J.*, 1996, 2, 481–486.
- 21 (a) G. R. Desiraju and A. Gavezzotti, *Acta Crystallogr., Sect. B: Struct. Sci.*, 1989, 45, 473–482; (b) C. A. Hunter and J. K. M. Sanders, *J. Am. Chem. Soc.*, 1990, 112, 5525–5534.
- 22 Cerius² ® version 3.8. <http://www.accelrys.com>.
- 23 (a) S. F. Alshahateet, R. Bishop, D. C. Craig and M. L. Scudder, *CrystEngComm*, 2001, 3(55), 264–268; (b) S. F. Alshahateet, R. Bishop, D. C. Craig and M. L. Scudder, *Cryst. Growth Des.*, 2010, 10, 1842–1847; (c) J. Ashmore, R. Bishop, D. C. Craig and M. L. Scudder, *J. Inclusion Phenom. Macrocyclic Chem.*, 2011, 71, 297–302.
- 24 R. Bishop, Enantiomeric Ordering and Separation During Molecular Inclusion, in *Separations and Reactions in Organic Supramolecular Chemistry*, ed. F. Toda and R. Bishop, Wiley, Chichester, 2004, ch. 2, pp. 33–60.
- 25 (a) R. Bishop, I. G. Dance and S. C. Hawkins, *J. Chem. Soc., Chem. Commun.*, 1983, 889–891; (b) S. C. Hawkins, M. L. Scudder, D. C. Craig, A. D. Rae, R. B. Abdul Raof, R. Bishop and I. G. Dance, *J. Chem. Soc., Perkin Trans. 2*, 1990, 855–870; (c) S. C. Hawkins, R. Bishop, I. G. Dance, T. Lipari, D. C. Craig and M. L. Scudder, *J. Chem. Soc., Perkin Trans. 2*, 1993, 1729–1735.
- 26 S. F. Alshahateet, K. Nakano, R. Bishop, D. C. Craig, K. D. M. Harris and M. L. Scudder, *CrystEngComm*, 2004, 6, 5–10.
- 27 S. F. Alshahateet, T. T. Ong, R. Bishop, F. Kooli and M. Messali, *Cryst. Growth Des.*, 2006, 6, 1676–1683.
- 28 J. Ashmore, R. Bishop, D. C. Craig and M. L. Scudder, *CrystEngComm*, 2008, 10, 131–137.
- 29 J. Ashmore, R. Bishop, D. C. Craig and M. L. Scudder, *CrystEngComm*, 2006, 8, 923–930.
- 30 SMART and SAINT, *Software Reference Manuals, Version 4.0*, Siemens Energy and Automation, Inc., Analytical Instrumentation, Madison, WI, USA, 1996.
- 31 G. M. Sheldrick, *SADABS: Software for empirical absorption correction*, University of Göttingen, Germany, 1996.
- 32 SHELXTL, *Reference Manuals Version 5.03*, Siemens Energy and Automation Inc., Analytical Instrumentation, Madison, WI, USA, 1996.
- 33 A. K. Rappe and W. A. Goddard, *J. Phys. Chem.*, 1991, 95, 3358–3363.